

RESEARCH ARTICLE

Mutation Analysis in Costello Syndrome: Functional and Structural Characterization of the *HRAS* p.Lys117Arg Mutation

Ellen Denayer,¹ Annabel Parret,² Magdalena Chmara,^{1,3} Suzanne Schubert,⁴ Annick Vogels,¹ Koen Devriendt,¹ Jean-Pierre Frijns,¹ Vladimir Rybin,² Thomy J. de Ravel,¹ Kevin Shannon,⁴ Jan Cools,^{1,5} Klaus Scheffzek,^{2*} and Eric Legius,^{1*}

¹Department of Human Genetics, Catholic University of Leuven, Leuven, Belgium; ²Structural and Computational Biology and Developmental Biology Units, European Molecular Biology Laboratory (EMBL), Heidelberg, Germany; ³Department of Biology and Genetics, Medical University of Gdansk, Gdansk, Poland; ⁴Department of Pediatrics and Comprehensive Cancer Center, University of California, San Francisco, California; ⁵Flanders Interuniversity Institute for Biotechnology (VIB), Catholic University of Leuven, Leuven, Belgium

Communicated by David E. Goldgar

Costello syndrome is a mental retardation syndrome characterized by high birth weight, postnatal growth retardation, coarse face, loose skin, cardiovascular problems, and tumor predisposition. De novo heterozygous missense mutations in *HRAS* codon 12 and 13 disturbing the intrinsic GTP hydrolysis cause Costello syndrome. We report a patient with typical Costello syndrome and a novel heterozygous missense mutation in codon 117 (c.350A>G, p.Lys117Arg) of the *HRAS* gene, resulting in constitutive activation of the RAS/MAPK pathway similar to the typical p.Gly12Ser and p.Gly12Ala mutations. Recombinant *HRAS* p.Lys117Arg demonstrates normal intrinsic GTP hydrolysis and responsiveness to GTPase-activating proteins, but the nucleotide dissociation rate is increased 80-fold. Consistent with the biochemical data, the crystal structure of the p.Lys117Arg mutant indicates an altered interaction pattern of the side chain that is associated with unfavorable nucleotide binding properties. Together, these data show that a RAS mutation that only perturbs guanine nucleotide binding has similar functional consequences as mutations that impair GTP hydrolysis and causes human disease. *Hum Mutat* 29(2), 232–239, 2008. © 2007 Wiley-Liss, Inc.

KEY WORDS: *HRAS*; Costello syndrome; guanine dissociation; GTPase activity

INTRODUCTION

Costello syndrome (MIM# 218040) was described by Costello in 1971 and 1977 [Costello, 1971, 1977]. It is characterized by high birth weight, neonatal feeding problems, failure to thrive, redundant skin of the neck, palms, and soles, coarse facial features, short stature, relative macrocephaly, cardiac abnormalities, and tumor predisposition. The most frequent tumors observed in Costello syndrome are rhabdomyosarcoma, followed by neuroblastoma and bladder carcinoma [Gripp, 2005]. Most patients are mildly to moderately mentally retarded with IQs ranging from 25 to 85 [Hennekam, 2003].

Costello syndrome has overlapping phenotypic features with Noonan syndrome (MIM# 163950) and cardio-facio-cutaneous (CFC) syndrome (MIM# 115150). In 50% of Noonan individuals missense mutations in the *PTPN11* gene, which encodes the tyrosine phosphatase SHP-2 are found [Tartaglia et al., 2001]. These are gain-of-function mutations, which result in enhanced phosphatase activity and activation of the RAS/MAPK pathway [Niihori et al., 2005].

Ras proteins (*HRAS*, *KRAS*, *NRAS*, and *ERAS*) are encoded by protooncogenes that are mutated in ~30% of human tumors. Activated RAS recruits RAF kinase resulting in RAF activation.

Activated RAF kinase phosphorylates and activates MEK, which in turn activates ERK/MAPK and other effectors [Kolch, 2005].

The Supplementary Material referred to in this article can be accessed at <http://www.interscience.wiley.com/jpages/1059-7794/suppmat>.

Received 2 April 2007; accepted revised manuscript 21 June 2007.

*Correspondence to: Eric Legius, Department of Human Genetics, Catholic University of Leuven, Herestraat 49, 3000 Leuven, Belgium. E-mail: Eric.Legius@uz.kuleuven.ac.be; and Klaus Scheffzek, Structural and Computational Biology and Developmental Biology Units, European Molecular Biology Laboratory (EMBL), Meyerhofstrasse 1, 69117 Heidelberg, Germany. E-mail: scheffzek@embl.de
Ellen Denayer and Annabel Parret contributed equally to the work

Grant sponsor: Concerted Action Grant from the KULeuven; Grant sponsor: Interuniversity Attraction Poles Grant, Federal Office for Scientific, Technical and Cultural Affairs, Belgium (2002–2006); Grant number: P5/25; Grant sponsor: Fonds voor Wetenschappelijk Onderzoek-Vlaanderen (FWO); Grant number: G.0096.02; Grant sponsor: Belgische Federatie tegen Kanker; Grant number: SCIE2003-33; Grant sponsor: NIH; Grant number: CA72614; Grant sponsor: EU Grant 3D-Repertoire; Grant number: LSHG-CT-2005-512028.

DOI 10.1002/humu.20616

Published online 2 November 2007 in Wiley InterScience (www.interscience.wiley.com).

Using a candidate gene approach Aoki et al. [2005] found *de novo* heterozygous missense mutations in codon 12 and 13 of the *HRAS* gene (MIM#190020) in 12 individuals with Costello syndrome. Later reports confirmed the presence of *HRAS* mutations in approximately 85% of individuals with a clinical diagnosis of Costello syndrome [Estep et al., 2006; Gripp et al., 2006; Kerr et al., 2006; Zampino et al., 2007]. *HRAS* amino acids 12 and 13 are the most frequently mutated *HRAS* codons in human cancer. Mutations at these sites impair the intrinsic RAS GTPase activity and reduce responsiveness to GTPase-activating proteins (GAPs). As a consequence, these mutant RAS proteins accumulate in the active, GTP-bound conformation, which results in constitutive activation of downstream effectors [Bos, 1989; Oliva et al., 2004].

Recently, missense mutations in *KRAS*, *BRAF*, and its downstream effectors *MEK1* and *MEK2* have been described in CFC syndrome [Niihori et al., 2006; Rodriguez-Viciano et al., 2006; Schubbert et al., 2006]. Moreover, about 2% of *PTPN11*-negative Noonan syndrome patients have a *KRAS* mutation [Carta et al., 2006; Schubbert et al., 2006] and 10% show mutations in the *GnEF SOS1* [Roberts et al., 2007; Tartaglia et al., 2007].

We sequenced the *HRAS* gene in 11 individuals with a clinical diagnosis of Costello syndrome and found heterozygous missense mutations in eight. In one individual, we found a heterozygous missense mutation in codon 117 (c.350A>G, p.Lys117Arg). Here, we show that the p.Lys117Arg substitution does not alter either intrinsic Ras GTPase activity or responsiveness to GAPs, but results in constitutive activation of *HRAS* and downstream effectors by markedly increasing the rate of nucleotide dissociation. To gain further insight into the underlying mechanism, we solved the crystal structure of Lys117Arg *HRAS*, which infers that the substitution of Lys117 by Arg results in additional polar interactions with residues within the nucleotide-binding pocket that lead to unfavorable nucleotide binding.

MATERIALS AND METHODS

Case Report

The patient was born at a gestational age of 38 weeks. Pregnancy was complicated by polyhydramnios. Her birth weight was 3,250 g (75th centile), length 51 cm (between the 75th and 90th centile), and head circumference 35 cm (between the 75th and 90th centile). There was no hypoglycemia at birth. Poor feeding and swallowing resulted in failure to thrive necessitating nasogastric tube feeding for several months and followed by a gastrostomy from the age of 6 months. Dysmorphic features included deep-set eyes, short eyelids, a long columella, and deep creases of the palms. Echocardiography revealed hypertrophic cardiomyopathy. At the age of 3 months a tracheostomy was performed because of severe laryngotracheomalacia and upper airway infections. She was hypotonic, moderately mentally retarded with a friendly personality, and no autistic or other behavior abnormalities were present. She could sit at the age of 2 years and walk alone at the age of 5 years. At the age of 6 years, no papillomas or other tumors were present, length (96.5 cm) and weight (15.3 kg) were below the third centile and head circumference (51.5 cm) was at the 50th centile.

Mutation Analysis

Genomic DNA was extracted from blood lymphocytes using standard techniques. *HRAS* exon 1 and 2 were amplified using the primer pair 5′GTGGGTTTGCCCTTCAGAT3′ and 5′ACATGC CAGAGAGGACAG3′. For exon 3 and *IDX* we used the

following primers: 5′CTGTCCTCTCTGCGCATGT3′ and 5′CTG TGTCGGCCCCAGGACT3′. Exon 4 was amplified with primers 5′AGGCTTGATCCCACAGCA3′ and 5′CCTCCATGTCCTGA GCTTGT3′. PCR products were purified using the QIAquick PCR purification kit (Qiagen Benelux, Venlo, The Netherlands) and sequenced using the Cycle Sequencing Big Dye Terminator v.3.1 kit (Applied Biosystems, Foster City, CA) and an ABI PRISM 3100 Genetic Analyzer (Applied Biosystems). DNA mutation numbering was based on the cDNA sequence with +1 corresponding to the A of the ATG translation initiation codon in the reference sequence (GenBank accession code: NM_005343.2). For protein numbering the initiation codon is codon 1.

HRAS Expression Constructs

Wild-type *HRAS* cDNA was amplified using the primer pair 5′TGGAGATCTGAGGAGCGATGACGGAATATAA3′ and 5′TGGGAATTCTCAGGAGAGCACACACTTGC3′ and cloned in a pGEMTeasy vector (Promega, Madison, WI). After plasmid DNA extraction and sequencing, this construct was used as a template in PCR reactions to generate the Gly12Ser, Gly12Ala, and Lys117Arg mutants using the primers 5′TGGAGATCTGAG GAGCGATGACGGAATATAAGCTGGTGGTGGTGGGGCCGCC GCCGGTGT3′, 5′TGGAGATCTGAGGAGCGATGACGGAAT ATAAGCTGGTGGTGGTGGGGCCGCCAGCCGTGT3′, 5′GCCA GGTCACACCTGTTCCCCACCAGCACCC3′, and 5′GGTGTCTG GTGGGAACAGGTGTGACCTGCG3′. These PCR-products were digested with the *EcoRI* and *BglIII* restriction enzymes and cloned into the pMSCV puro vector (Clontech Laboratories, Mountain View, CA). Plasmid DNA was extracted with the Qiagen Plasmid midi kit (Qiagen) and sequence-verified.

HRAS Expression Studies

Human embryonal kidney (HEK) 293 T cells were cultured in Dulbecco's Modified Eagle's Medium (DMEM; Gibco, Invitrogen, Carlsbad, CA) with 10% fetal calf serum (FCS). They were transiently transfected using FuGENE 6 transfection reagent (Roche Diagnostics, Basel, Switzerland) with the pMSCV vectors encoding wild-type *HRAS* cDNA and the Gly12Ala, Gly12Ser, and Lys117Arg constructs. After 24 hr cells were either lysed in 1% Triton X buffer containing 1 mM Na₂EDTA, 1 mM ethylene glycol-bis-(beta-aminoethylether)-N,N,N',N'-tetraacetic acid (EGTA), 50 mM NaF, 5 mM Na₃VO₄, 20 μM phenylarsine oxide (PAO), and protease inhibitor cocktail tablets (Complete; Roche), or starved overnight in serum free medium and then stimulated with acidic fibroblast growth factor (aFGF) (10 μg/ml) for 0 and 10 minutes, respectively, and then lysed. Proteins were separated by NuPAGE NOVEX Bis-Tris gel 4-12% (Invitrogen) electrophoresis and transferred to a Hybond-P (GE Healthcare Bio-Sciences, Uppsala, Sweden) membrane polyvinylidene difluoride (PVDF). After blocking with 5% nonfat milk, membranes were incubated overnight with monoclonal rabbit phosphorylated ERK (P-ERK) or phosphorylated MEK (P-MEK), incubated with horseradish peroxidase-conjugated anti-rabbit antibodies for 1 hr, and visualized with enhanced chemiluminescence. After stripping, membranes were also incubated with polyclonal rabbit *HRAS* antibody and β-actin. All antibodies were obtained from Santa Cruz Biotechnologies (Santa Cruz, CA), except for β-actin (Sigma-Aldrich, St. Louis, MO).

RAS-GTP was measured using the RAS Activation Assay kit (Upstate Biotechnology, Lake Placid, NY) according to the manufacturer's instructions. Briefly, cells were lysed in

magnesium-containing lysis buffer (MLB) and proteins were incubated with RAS binding domain of RAF1 (RAF1-RBD) agarose for 2 hr. After three washes, Western blotting was performed as described above using anti-pan-RAS antibody (Upstate).

Retrovirus Production and Transduction of Ba/F3 Cells

Retroviral stocks were generated by transient cotransfection of 293 T cells with pMSCV puro vectors containing HRAS wild-type, Gly12Ala, Gly12Ser, and Lys117Arg constructs with a packaging construct (p.IK6.1MCV.ecopac.UTd; Cell Genesys, San Francisco, CA), providing sequences necessary for retrovirus production. At 48 hr after transfection, virus-containing supernatant was collected, filtered (0.45- μ m filter), and stored at -70°C . Ba/F3 cells were transduced with 1 ml of retroviral supernatant containing MSCVpuro constructs and grown in RPMI 1640 (Gibco, Invitrogen) containing 10% FCS, 1 $\mu\text{g}/\text{ml}$ interleukin-3 (IL-3), and 8 $\mu\text{g}/\text{ml}$ polybrene (Sigma). After 24 hr, selection with 2.5 $\mu\text{g}/\text{ml}$ puromycin was started. After 6 days of selection, cells were washed twice with D-PBS and counted with a Vi-cell counter (Beckman Coulter, Fullerton, CA). Cells were resuspended in 10 ml RPMI +10% FCS to a final concentration of 100,000 cells/ml. For each construct and for noninfected Ba/F3 cells, two separate culture conditions were initiated, one with and one without IL-3. From then on, cell counts were analyzed for 3 consecutive days. This experiment was repeated thrice.

Recombinant Protein Expression and Purification

The Lys117Arg mutation was introduced into *ptac-Hras*' [John et al., 1989] encoding C-terminally truncated HRAS(1–166) by quick change mutagenesis using primers 5'CTGGTGGGGAACCGTTGTGACCTGG3' and 5'CCAGGTCACAACGGTCCCCCACCAG3'. Truncated RAS was used since it can be crystallized more conveniently and it preserves the basic biochemical properties of the full-length protein. The mutation was sequence-verified and the plasmid was transformed to *E. coli* expression host CK600K. Protein was purified following previously published procedures except for the addition of 10% glycerol to all buffers to prevent protein precipitation [Tucker et al., 1986]. In addition, protein was concentrated using Amicon Centrifugal Filter Units MWCO 10 kDa (Millipore, Billerica, MA) instead of ammonium sulfate precipitation, allowing more rapid purification. Q sepharose fast flow resin (GE Healthcare Bio-Sciences) was used for anion exchange and a superdex75 (GE Healthcare Bio-Sciences) for size-exclusion chromatography, resulting in >95% pure protein. Protein concentration was estimated by measuring the absorbance at 280 nm, employing the calculated molar extinction coefficient of 13,535 $\text{M}^{-1}\text{cm}^{-1}$ (calculated with the ExPaSy proteomics server; www.expasy.ch). The guanosine diphosphate (GDP) load of the pure protein was confirmed using an HPLC C18 reverse column as described previously [Smith and Rittinger, 2002].

Intrinsic and GAP-Stimulated GTP Hydrolysis

These assays have been described elsewhere [Bollag and McCormick, 1991, 1995]. Briefly, recombinant GAP-related domain (GRD) proteins from p120 GAP and neurofibromin were produced in *E. coli*. Incubation of 200 nM of each recombinant HRAS protein preloaded with (γ - ^{32}P)GTP without (intrinsic GTPase activity assay) or with GRD proteins (GAP assays) took place at room temperature. The reactions were terminated by quenching with 5 mM sodium silicotungstate/1 mM H_2SO_4 . Isobutanol/toluene and 5% ammonium molybdate/2 M H_2SO_4

were used for extraction of the free phosphate from the aqueous layer, which was quantified in a scintillation counter. Intrinsic GTP hydrolysis was measured over a time course from 10 to 80 minutes whereas GAP activity was assessed at 8 minutes. All assays were performed in duplicate.

GTP Exchange Assay

Recombinant HRAS proteins (500 nM) were labeled with (α - ^{32}P)GTP in 5 mM EDTA at room temperature. Aliquots were removed from the loading reaction and placed into 20 mM HEPES pH 7.3, 50 mM NaCl, 2 mM MgCl_2 , 2 mM dithiothreitol (DTT), 0.2 mg/ml bovine serum albumin (BSA), and 0.2 mM (excess) unlabeled GTP to allow guanine nucleotide exchange for the designated time points. The amount of labeled guanine nucleotide bound to HRAS was determined by vacuum filtration through nitrocellulose filters (0.22 μm pore size) and liquid scintillation counting.

Kinetics of Nucleotide Dissociation

A total of 5 nmol HRAS Lys117Arg was incubated in a solution containing 64 mM TrisHCl (pH 7.6), 1 mM DTT, 10% glycerol, 2 mM EDTA, and 50 μM *N*-methylanthraniloyl (mant)-nucleotide (Jena Biosciences, Jena, Germany) at room temperature to allow exchange of GDP to mant-GDP according to Ahmadian et al. [2002]. Nucleotide exchange was stopped after 1 hr by adjusting the MgCl_2 concentration to 10 mM and incubating the reaction for 5 minutes on ice. The mixture was purified from EDTA and excess nucleotide using a Nap-5 column (GE Healthcare Bio-Sciences). Protein was eluted with 1 ml 64 mM TrisHCl pH 7.6, 10 mM MgCl_2 , 1 mM DTT, 10% glycerol, 10 mM MgCl_2 buffer, and fractions containing protein were identified using the Bradford assay. Fractions containing HRAS protein were pooled and protein concentration was estimated. For dissociation assays, 2 μM protein was mixed in a quartz cuvette in a total volume of 150 μl with a 500-fold molar excess of unlabelled GTP. All reactions were conducted at 20°C and fluorescence was monitored with an excitation wavelength of 355 nm and an emission wavelength of 445 nm (4-nm slit widths on an Aminco-Bowman spectrofluorimeter [SLM Aminco, Urbana, IL]). Dissociation was measured for 30 minutes with 10-second intervals.

Crystallization and Structure Determination

Crystals were grown at room temperature ($\sim 20^{\circ}\text{C}$) by the vapor diffusion technique in hanging or sitting drops by mixing 1 μl of protein (15 mg/ml in 64 mM TrisHCl pH 7.6, 10 mM MgCl_2 , 1 mM DTT, 10% glycerol, pH 7.6) and 1 μl from a total reservoir (36–38% polyethylene glycol (PEG)3350, 50 mM TrisHCl pH 7.6) of 100 μl . The rhombohedral crystals were transferred to reservoir solution and flash-frozen in liquid nitrogen. A data set to 1.49 \AA resolution was collected on beamline ID29 at the European Synchrotron Radiation Facility (ESRF, Grenoble, France). The structure was solved by molecular replacement with the program PHASER [McCoy et al., 2005] using the coordinates of the GDP-loaded wild-type protein (Protein Data Bank accession code 4Q21; www.rcsb.org/pdb/home/home.do) as search model. Data processing and scaling were carried out with XDS (version: May 2005) [Kabsch, 1993]. Several rounds of alternating refinement and manual rebuilding using the programs REFMAC5 [Murshudov et al., 1997] and COOT [Emsley and Cowtan, 2004], respectively, were performed. Data collection and refinement statistics are summarized in Supplementary Table S1TBL S1 (available online at <http://www.interscience.wiley.com/jpages/1059-7794/suppmat>).

Structural alignments and visualization were created using the program PyMOL, version 0.99 (PyMOL; <http://pymol.sourceforge.net>) [DeLano, 2002].

RESULTS

Mutation Analysis

A c.350A>G transition resulting in the p.Lys117Arg mutation was found in the patient DNA (Fig. 1A) but not in DNA from both parents.

HRAS Expression Studies

To explore the functional consequences of the Lys117Arg mutant, we assayed ERK and MEK phosphorylation in transfected 293 T by Western blotting. Levels of phosphorylated MEK, ERK, and Ras-GTP are elevated in cells transfected with the HRAS Lys117Arg construct compared to cells expressing wild-type HRAS, and are similar to those observed in 293 T cells transfected with known activating mutations (HRAS Gly12Ser and HRAS Gly12Ala) (Fig. 2A).

After overnight starvation, 293 T cells expressing wild-type HRAS demonstrate lower levels of phosphorylated ERK (pERK) than cells transfected with Lys117Arg, Gly12Ala or Gly12Ser mutant proteins (Fig. 2B). FGF stimulation induced robust ERK

phosphorylation in transfected 293 T cells after 10 minutes that was equivalent in cells expressing wild-type and mutant HRAS proteins.

Proliferation of Ba/F3 Cells

To determine the effect of HRAS Lys117Arg on proliferation of growth factor-dependent hematopoietic cells, we transduced IL-3-dependent Ba/F3 cells with HRAS constructs. Ba/F3 cells expressing HRAS Lys117Arg, HRAS Gly12Ser, or HRAS Gly12Ala continued to proliferate after IL-3 withdrawal whereas cells expressing wild-type HRAS did not proliferate in the absence of IL-3 (Fig. 3A). As expected, there were no differences in proliferation rate between parental Ba/F3 cells and Ba/F3 cells expressing HRAS wild-type, Gly12Ala, Gly12Ser, or Lys117Arg constructs in the presence of IL-3 (Fig. 3B).

Biochemical Analysis of HRAS Lys117Arg

To establish the biochemical consequences of the Lys117Arg mutation, we investigated the ability of C-terminally truncated recombinant HRAS Lys117Arg to release nucleotide in two ways. First, we measured nucleotide displacement by incubating GDP-loaded HRAS wild-type and HRAS Lys117Arg with an excess of fluorescence-labeled GDP. As shown in Figure 4A, HRAS Lys117Arg has a considerably higher off-rate for GDP

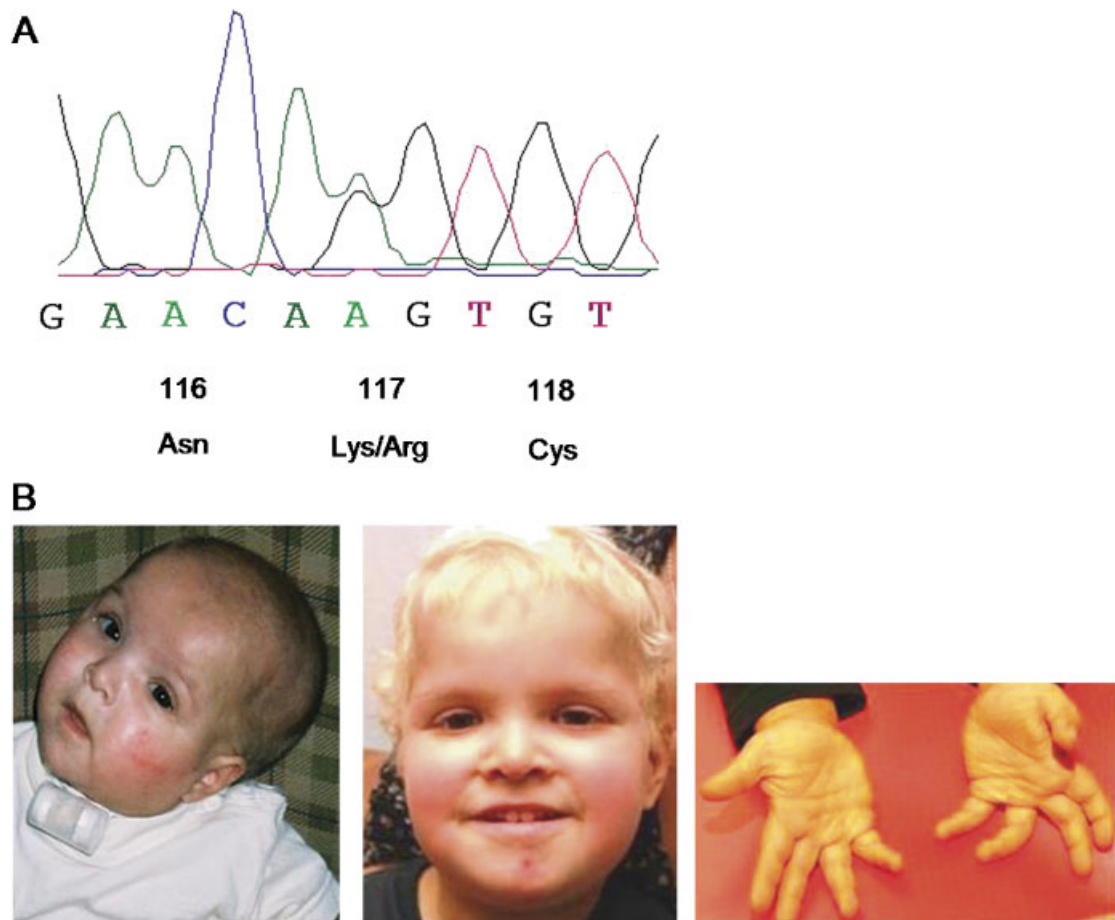


FIGURE 1. **A:** Sequencing data: *HRAS* codons 116, 117, 118 from the reported patient showing the c.350A>G transition resulting in the p.Lys117Arg mutation. DNA mutation numbering was based on cDNA sequence with +1 corresponding to the A of the ATG translation initiation codon in the reference sequence (GenBank accession number: NM_005343.2). For protein numbering the initiation codon is codon 1. **B:** Photographs of the patient. [Color figure can be viewed in the online issue, which is available at www.interscience.wiley.com.]

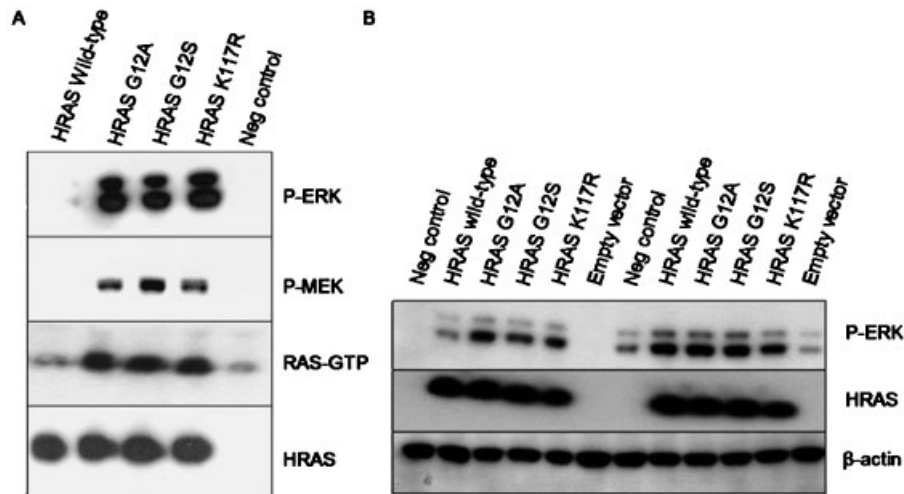


FIGURE 2. Functional characterization of HRAS Lys117Arg. **A:** P-ERK, P-MEK, and Ras-GTP in 293 T cells transfected with HRAS wild-type, HRAS Gly12Ala (G12A), Gly12Ser (G12S), and Lys117Arg (K117R) constructs. HRAS protein levels are similar in 293 T cells expressing each protein and are used as a loading control. Untransfected 293 T cells, used as a negative control, show no endogenous HRAS expression. **B:** P-ERK in 293 T cells transfected with HRAS wild-type, HRAS Gly12Ala, Gly12Ser, and Lys117Arg constructs after starvation (lanes 2–5) and 10 minutes after stimulation with aFGF (10 μ g/ml) (lanes 8–11). β -actin is shown as a loading control.

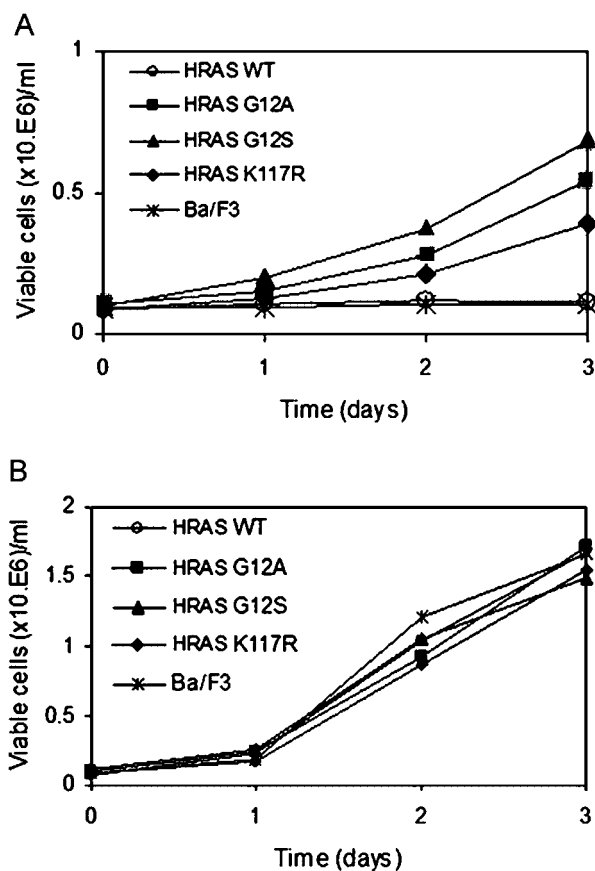


FIGURE 3. Growth-factor independent proliferation of Ba/F3 cells. **A:** Ba/F3 cells expressing HRAS Lys117Arg (K117R), HRAS Gly12Ala (G12A), or HRAS Gly12Ser (G12S) continue to proliferate after IL-3 removal, whereas cells expressing wild-type (WT) HRAS stop proliferating in the absence of IL-3. **B:** In the presence of IL-3 there is no difference in proliferation rate between noninfected Ba/F3 cells and Ba/F3 cells expressing HRAS wild-type, Gly12Ala, Gly12Ser, or Lys117Arg constructs.

compared to the wild-type protein. Filter binding assays to measure guanine nucleotide dissociation of (γ - 32 P)GTP over time from HRAS wild-type and HRAS Lys117Arg were also performed. These studies confirmed a markedly elevated rate of guanine nucleotide dissociation from the mutant protein (data not shown). HRAS wild-type and HRAS Lys117Arg were also loaded with (α - 32 P)GTP to assess intrinsic GTP hydrolysis and responsiveness to GTPase activating proteins. HRAS Lys117Arg demonstrated normal intrinsic GTPase activity (Fig. 4B) and also responded normally to the GAP-related domains of neurofibromin and p120 GAP (Fig. 4C and D).

Structural Analysis of HRAS Lys117Arg

To investigate the properties of the HRAS Lys117Arg mutant at a structural level, the crystal structure of GDP-bound HRAS Lys117Arg was determined (Supplementary table S1) and was found to be similar to that of HRAS wild-type (root mean square deviation of 0.5 \AA when comparing 166 corresponding C α -atoms). The aliphatic portion of Arg117 partly aligns with that of Lys117 of the wild-type protein. Its guanidinium group is stabilized by interactions with the P-loop (Gly13, main-chain CO) and additionally with Asn85 located at the N-terminal end of one of the core helices (α 3) of the G-domain (Fig. 5). Taken together, this appears to induce a conformation of the nucleotide binding pocket that is less favorable for nucleotide binding, which is consistent with the biochemical data.

DISCUSSION

HRAS mutations in amino acids 12 and 13 are found in 85 to 90% of Costello syndrome patients. Whereas Gly¹² and Gly¹³ are common targets of cancer-associated RAS mutations, a Lys¹¹⁷ mutation (K117E) has only been described in a myeloma cell line [Crowder et al., 2003]. The only other Costello syndrome patient with a p.Lys117Arg mutation was described to be unusual because of microretrognathism and less pronounced palmar and plantar creases. That patient also exhibited autistic behavior with verbal

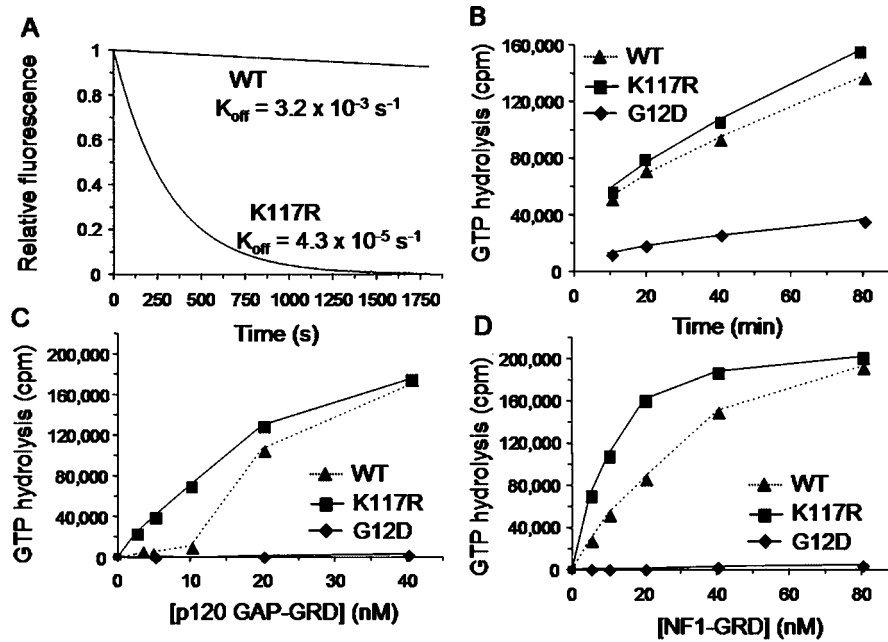


FIGURE 4. Intrinsic GDP dissociation and hydrolysis rates of wild-type and mutant HRAS proteins. **A:** Nucleotide dissociation rates were measured by following the decrease in fluorescence of the nucleotide analog mant-GDP [Ahmadian et al., 2002]. Data are representative of three independent experiments and were fitted to a single decaying exponential using the Origin 7.5 software. GDP dissociation is 80-fold faster for Lys117Arg (K117R) compared to wild-type (WT) protein. **B:** Intrinsic GTP hydrolysis measured as the number of counts per minute (cpm) released over time. **C,D:** Phosphate release by wild-type and mutant HRAS proteins (measured as cpm) in response to 5–80 nM of neurofibromin (NF1) (C) and 2.5–40 nM of p120 (D) GRDs. No significant effect of the Lys117Arg mutation was observed on intrinsic and GAP-stimulated GTP hydrolysis. Mutant Gly12Asp (G12D) KRAS (B) or Gly12Asp HRAS (C,D) were included as a positive control for impaired GTP hydrolysis [Schubbert et al., 2006].

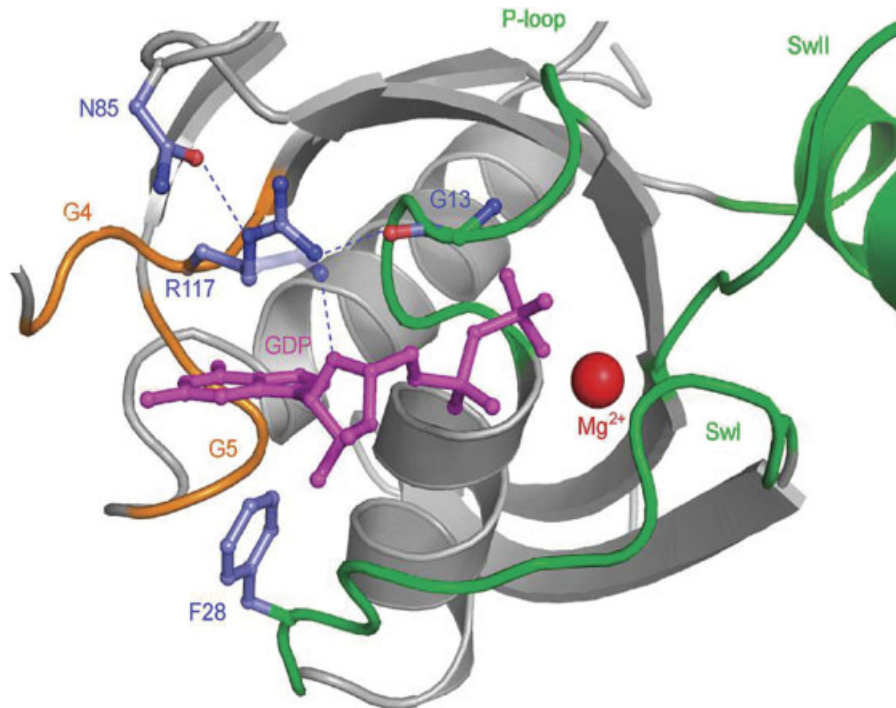


FIGURE 5. Structure of the HRAS Lys117Arg variant. Close-up view of the nucleotide-binding region of Lys117Arg. The guanidinium group of Arg117 (R117) undergoes an additional interaction with Asn85 (N85) when compared with the Lys117 from the wild-type protein (superimposed in semitransparent). The conserved GTP/GDP binding motifs G4, G5 (orange), and the P-loop (blue) are indicated. Swl [residues 32–38] and Swll [residues 59–67] denote the switch regions, which undergo large conformational changes upon transition between active GTP- and inactive GDP-bound conformations. Polar interactions are indicated as dashed lines. The interaction pattern apparently stabilizes the conformation of Arg117 but is unfavorable for nucleotide binding (see Structural Analysis of HRAS Lys117Arg).

stereotypes and hand biting [Kerr et al., 2006]. By contrast the phenotype of the patient reported here was similar to the features seen in the patients with mutations in codon 12 or 13 of *HRAS*, although the craniofacial features are rather mild.

The c.350A>G transition results in a lysine-to-arginine substitution at position 117, which is part of the N=Asn, K=Lys, X=any amino acid, D=Asp (=nucleotide binding consensus sequence=residues 116–119 (NKXD)-fingerpoint motif, important for base binding of the nucleotide [Pai et al., 1990]. This mutant *HRAS* protein was found to activate the RAF/MEK/ERK cascade in 293 T cells and confer a phenotype of growth factor (IL-3) independent proliferation in Ba/F3 cells. Thus, although lysine and arginine belong to the same amino acid class, the mutation results in constitutive activation of *HRAS*. In the structure of *HRAS*, Lys117 stabilizes nucleotide binding by its aliphatic portion interacting with the base, and its amino group interacting with ribose oxygen O4 and with a main chain segment (Gly13, CO) from the phosphate binding loop (P-loop). We have studied the effect on the protein structure by crystallographic analysis of GDP-bound *HRAS* Lys117Arg. While loss of critical interactions with the nucleotide is unlikely to explain the reduced binding affinities, subtle steric rearrangements as a consequence of the larger side chain with an additional polar interaction most likely introduce secondary features destabilizing nucleotide binding. Lys117 to Arg and other substitutions within the NKXD region have been shown to result in 2,000-fold reduced GTP binding affinity for Lys117Arg. Moreover *HRAS* Lys117Arg demonstrated similar transforming activity in fibroblasts as GTPase impaired mutants [Der et al., 1988]. Despite a high rate of guanine nucleotide dissociation, we found that the intrinsic GTPase activity of *HRAS* Lys117Arg and the responsiveness of this mutant protein to the GAP domains of neurofibromin and p120 GAP were normal. Considering that the intracellular concentration of GTP is higher than that of GDP (GTP:GDP ratio of 25:1) [Proud, 1986] mutant RAS proteins with high rates of guanine nucleotide dissociation and reassociation are predicted to accumulate in the active GTP-bound conformation in vivo [Walter et al., 1986]. Consistent with this idea, another Ras mutant in which the guanine base stabilizing Phe28 has been replaced by leucine demonstrates a dramatic increase in the rate of nucleotide dissociation and induces neurite differentiation in PC12 cells, while responding normally to RasGAP [Reinstein et al., 1991].

In summary, we report the first comprehensive analysis of a novel germ line RAS mutation identified in a human developmental disorder that includes solving the crystal structure of the mutant protein bound to guanine nucleotide. Whereas previous studies of RAS mutations found in cancer and developmental disorders have focused on how these alterations perturb the GTPase switch, Carta et al. [2006] have speculated that disease-associated amino acid substitutions at codons 152 and 153 might activate KRAS by increasing the rate of nucleotide exchange. Our analysis of *HRAS* Lys117Arg provides the first direct evidence that amino acid substitutions that have no effect on enzymatic activity are sufficient to cause disease.

Data deposition: The atomic coordinates and structure factors of the GDP-bound H-RasK117R protein have been deposited in the Protein Data Bank (www.rcsb.org) with accession code 2QUZ.

ACKNOWLEDGMENTS

We thank Kanchan Anand and the staff at beamline ID29 of the European Synchrotron Radiation Facility (ESRF), Grenoble,

France, for help and technical support during data collection, and Gideon Bollag for providing recombinant neurofibromin and p120 GAP proteins. This work is supported in part by the Fonds voor Wetenschappelijk Onderzoek-Vlaanderen (G.0096.02 to E.L.), the Belgische Federatie tegen Kanker (SCIE2003-33 to E.L.), E.D. is a predoctoral researcher (Aspirant van het Fonds voor Wetenschappelijk Onderzoek-Vlaanderen [FWO]), J.C. is a postdoctoral researcher, and E.L. is a part-time clinical researcher of the FWO. A.P. was supported by the EU grant 3D-Repertoire contract no. LSHG-CT-2005-512028. M.C. was supported by the Marie Curie European Community fellowship (Contract HPMT-CT2001-00273).

REFERENCES

- Ahmadian MR, Wittinghofer A, Hermann C. 2002. Fluorescence methods in the study of small GTP-binding proteins. *Methods Mol Biol* 189: 45–63.
- Aoki Y, Niihori T, Kawame H, Kurosawa K, Ohashi H, Tanaka Y, Filocamo M, Kato K, Suzuki Y, Kure S, Matsubara Y. 2005. Germline mutations in *HRAS* proto-oncogene cause Costello syndrome. *Nat Genet* 37: 1038–1040.
- Bollag G, McCormick F. 1991. Differential regulation of rasGAP and neurofibromatosis gene product activities. *Nature* 351:576–579.
- Bollag G, McCormick F. 1995. Intrinsic and GTPase-activating protein-stimulated Ras GTPase assays. *Methods Enzymol* 255:161–170.
- Bos JL. 1989. Ras oncogenes in human cancer: a review. *Cancer Res* 49: 4682–4689.
- Carta C, Pantaleoni F, Bocchinfuso G, Stella L, Vasta I, Sarkozy A, Digilio C, Palleschi A, Pizzuti A, Grammatico P, Zampino G, Dallapiccola B, Gelb BD, Tartaglia M. 2006. Germline missense mutations affecting KRAS isoform B are associated with a severe Noonan syndrome phenotype. *Am J Hum Genet* 79:129–135.
- Costello JM. 1971. A new syndrome. *NZ Med J* 74:374.
- Costello JM. 1977. A new syndrome: mental subnormality and nasal papillomata. *Aust Paediatr J* 13:114–118.
- Crowder C, Kopantzev E, Williams K, Lengel C, Miki T, Rudikoff S. 2003. An unusual H-Ras mutant isolated from a human multiple myeloma line leads to transformation and factor-independent cell growth. *Oncogene* 22:649–659.
- DeLano WL. 2002. The PyMOL molecular graphics system. San Carlos, CA: DeLano Scientific.
- Der CJ, Weissman B, MacDonald MJ. 1988. Altered guanine nucleotide binding and H-ras transforming and differentiating activities. *Oncogene* 3:105–112. (This reference can be found in ISI Web of knowledge ISSN number: 0950-9232.)
- Emsley P, Cowtan K. 2004. COOT: model-building tools for molecular graphics. *Acta Crystallogr D Biol Crystallogr* 60:2126–2132.
- Estep AL, Tidyman WE, Teitell MA, Cotter PD, Rauken KA. 2006. *HRAS* mutations in Costello syndrome: detection of constitutional activating mutations in codon 12 and 13 and loss of wild-type allele in malignancy. *Am J Med Genet A* 140:8–16.
- Gripp KW. 2005. Tumor predisposition in Costello syndrome. *Am J Med Genet C Semin Med Genet* 137:72–77.
- Gripp KW, Lin AE, Stabley DL, Nicholson L, Scott CL, Jr, Doyle D, Aoki Y, Matsubara Y, Zackai EH, Lapunzina P, Gonzalez-Meneses A, Holbrook J, Agresta CA, Gonzalez IL, Sol-Church K. 2006. *HRAS* mutation analysis in Costello syndrome: genotype and phenotype correlation. *Am J Med Genet A* 140:1–7.
- Hennekam RC. 2003. Costello syndrome: an overview. *Am J Med Genet C Semin Med Genet* 117:42–48.
- John J, Schlichting I, Schiltz E, Rosch P, Wittinghofer A. 1989. C-terminal truncation of p21H preserves crucial kinetic and structural properties. *J Biol Chem* 264:13086–13092.
- Kabsch W. 1993. Automatic processing of rotation diffraction data from crystals of initially unknown symmetry and cell constants. *J Appl Crystallogr* 26:795–800.

- Kerr B, Delrue MA, Sigaudy S, Perveen R, Marche M, Burgelin I, Stef M, Tang B, Eden OB, O'Sullivan J, Sandre-Giovannoli A, Reardon W, Brewer C, Bennett C, Quarell O, M'Cann E, Donnai D, Stewart F, Hennekam R, Cave H, Verloes A, Philip N, Lacombe D, Levy N, Arveiler B, Black G. 2006. Genotype–phenotype correlation in Costello syndrome: HRAS mutation analysis in 43 cases. *J Med Genet* 43:401–405.
- Kolch W. 2005. Coordinating ERK/MAPK signalling through scaffolds and inhibitors. *Nat Rev Mol Cell Biol* 6:827–837.
- McCoy AJ, Grosse-Kunstleve RW, Storoni LC, Read RJ. 2005. Likelihood-enhanced fast translation functions. *Acta Crystallogr D Biol Crystallogr* 61:458–464.
- Murshudov GN, Vagin AA, Dodson EJ. 1997. Refinement of macromolecular structures by the maximum-likelihood method. *Acta Crystallogr D Biol Crystallogr* 53:240–255.
- Niihori T, Aoki Y, Ohashi H, Kurosawa K, Kondoh T, Ishikiriya S, Kawame H, Kamasaki H, Yamanaka T, Takada F, Nishio K, Sakurai M, Tamai H, Nagashima T, Suzuki Y, Kure S, Fujii K, Imaizumi M, Matsubara Y. 2005. Functional analysis of PTPN11/SHP-2 mutants identified in Noonan syndrome and childhood leukemia. *J Hum Genet* 50:192–202.
- Niihori T, Aoki Y, Narumi Y, Neri G, Cave H, Verloes A, Okamoto N, Hennekam RC, Gillessen-Kaesbach G, Wiczorek D, Kavamura MI, Kurosawa K, Ohashi H, Wilson L, Heron D, Bonneau D, Corona G, Kaname T, Naritomi K, Baumann C, Matsumoto N, Kato K, Kure S, Matsubara Y. 2006. Germline KRAS and BRAF mutations in cardio-facio-cutaneous syndrome. *Nat Genet* 38:294–296.
- Oliva JL, Zarich N, Martinez N, Jorge R, Castrillo A, Azanedo M, Garcia-Vargas S, Gutierrez-Eisman S, Juarranz A, Bosca L, Gutkind JS, Rojas JM. 2004. The P34G mutation reduces the transforming activity of K-Ras and N-Ras in NIH 3T3 cells but not of H-Ras. *J Biol Chem* 279:33480–33491.
- Pai EF, Krengel U, Petsko GA, Goody RS, Kabsch W, Wittinghofer A. 1990. Refined crystal structure of the triphosphate conformation of H-ras p21 at 1.35 Å resolution: implications for the mechanism of GTP hydrolysis. *EMBO J* 9:2351–2359.
- Proud CG. 1986. Guanine nucleotides, protein phosphorylation and the control of translation. *Trends Biochem Sci* 11:73–77.
- Reinstein J, Schlichting I, Frech M, Goody RS, Wittinghofer A. 1991. p21 with a phenylalanine 28–leucine mutation reacts normally with the GTPase activating protein GAP but nevertheless has transforming properties. *J Biol Chem* 266:17700–17706.
- Roberts AE, Araki T, Swanson KD, Montgomery KT, Schiripo TA, Joshi VA, Li L, Yassin Y, Tamburino AM, Neel BG, Kucherlapati RS. 2007. Germline gain-of-function mutations in SOS1 cause Noonan syndrome. *Nat Genet* 39:70–74.
- Rodriguez-Viciana P, Tetsu O, Tidyman WE, Estep AL, Conger BA, Cruz MS, McCormick F, Rauen KA. 2006. Germline mutations in genes within the MAPK pathway cause cardio-facio-cutaneous syndrome. *Science* 311:1287–1290.
- Schubert S, Zenker M, Rowe SL, Boll S, Klein C, Bollag G, van dB, I, Musante L, Kalscheuer V, Wehner LE, Nguyen H, West B, Zhang KY, Siermans E, Rauch A, Niemeyer CM, Shannon K, Kratz CP. 2006. Germline KRAS mutations cause Noonan syndrome. *Nat Genet* 38:331–336.
- Smith SJ, Rittinger K. 2002. Preparation of GTPases for structural and biophysical analysis. *Methods Mol Biol* 189:13–24.
- Tartaglia M, Mehler EL, Goldberg R, Zampino G, Brunner HG, Kremer H, van dB, I, Crosby AH, Ion A, Jeffery S, Kalidas K, Patton MA, Kucherlapati RS, Gelb BD. 2001. Mutations in PTPN11, encoding the protein tyrosine phosphatase SHP-2, cause Noonan syndrome. *Nat Genet* 29:465–468.
- Tartaglia M, Pennacchio LA, Zhao C, Yadav KK, Fodale V, Sarkozy A, Pandit B, Oishi K, Martinelli S, Schackwitz W, Ustaszewska A, Martin J, Bristow J, Carta C, Lepri F, Neri C, Vasta I, Gibson K, Curry CJ, Siguero JP, Digilio MC, Zampino G, Dallapiccola B, Bar-Sagi D, Gelb BD. 2007. Gain-of-function SOS1 mutations cause a distinctive form of Noonan syndrome. *Nat Genet* 39:75–79.
- Tucker J, Sczakiel G, Feuerstein J, John J, Goody RS, Wittinghofer A. 1986. Expression of p21 proteins in *Escherichia coli* and stereochemistry of the nucleotide-binding site. *EMBO J* 5:1351–1358.
- Walter M, Clark SG, Levinson AD. 1986. The oncogenic activation of human p21ras by a novel mechanism. *Science* 233:649–652.
- Zampino G, Pantaleoni F, Carta C, Cobellis G, Vasta I, Neri C, Pogna EA, De Feo E, Delogu A, Sarkozy A, Atzeri F, Selicorni A, Rauen KA, Cytrynbaum CS, Weksberg R, Dallapiccola B, Ballabio A, Gelb BD, Neri G, Tartaglia M. 2007. Diversity, parental germline origin, and phenotypic spectrum of de novo HRAS missense changes in Costello syndrome. *Hum Mutat* 28:265–272.